Biophysical Chemistry 134 (2008) 246–253

Contents lists available at ScienceDirect

Biophysical Chemistry

journal homepage: http://www.elsevier.com/locate/biophyschem

Structural stability and reversible unfolding of recombinant porcine S100A12

A.F. Garcia [a], W. Garcia [a], M.C. Nonato [b], A.P.U. Araújo [a,*]

[a] Instituto de Física de São Carlos, Universidade de São Paulo, São Carlos, SP, Brazil
[b] Laboratório de Cristalografia de Proteínas, Departamento de Física e Química, Faculdade de Ciências Farmacêuticas de Ribeirão Preto—USP, Brazil

ARTICLE INFO

Article history:
Received 21 January 2008
Received in revised form 20 February 2008
Accepted 20 February 2008
Available online 29 February 2008

Keywords:
S100A12
Calcium-binding protein
S100 family, Circular dichroism (CD)
Fluorescence spectroscopy
Protein unfolding

ABSTRACT

Porcine S100A12 is a member of the S100 proteins, family of small acidic calcium-binding proteins characterized by the presence of two EF-hand motifs. These proteins are involved in many cellular events such as the regulation of protein phosphorylation, enzymatic activity, protein–protein interaction, Ca^{2+} homeostasis, inflammatory processes and intermediate filament polymerization. In addition, members of this family bind Zn^{2+} or Ca^{2+} with cooperative effect on binding. In this study, the gene sequence encoding porcine S100A12 was obtained by the synthetic gene approach using *E. coli* codon bias. Additionally, we report a thermodynamic study of the recombinant S100A12 using circular dichroism, fluorescence and isothermal titration calorimetry. The results of urea and temperature induced unfolding and refolding processes indicated a reversible two-state process. Also, the ANS fluorescence studies showed that in presence of divalent ions the protein exposes hydrophobic sites which could facilitate the interaction with other proteins and trigger the physiological responses.

1. Introduction

Calcium-binding proteins (CaBPs) are involved in the regulation of several biological processes. The basic structural and functional unit of CaBPs family is the EF-hand motif which is the target of intracellular calcium [1,2]. S100 proteins constitute the largest subfamily of EF-hand proteins. There are at least 25 members of low-molecular-weight (9–14 kDa) acidic calcium-binding proteins [3,4]. They interact in a Ca^{2+}-dependent or independent way with proteins involved in cell proliferation and differentiation, cellular architecture, signal transduction, and intracellular metabolism [4,5].

Most S100 proteins occur as non-covalent homodimers [6] and are characterized by the presence of two EF-hand motifs per monomer, which are ordered in N-terminal EF-hand (helix I–loop I–helix II) with a flexible linker region that connects helix II to helix III of the C-terminal EF-hand (helix III–loop II–helix IV). The linker region and C-terminal extension show the least amount of sequence conservation among S100 proteins [7,8]. Different conformational changes are triggered by calcium binding to S100 proteins in the two EF-hands, and they exhibit distinctive affinities for calcium [9]. The C-terminal EF-hand contains the canonical Ca^{2+}-binding loop common to all CaBPs. The N-terminal EF-hand of S100 proteins is distinguished from all other CaBPs [3,9]. Also, it undergoes a relatively small change in conformation, whereas the change in the C-terminal EF-hand is much larger. These large differences in the Ca^{2+} affinities indicate that S100 proteins are hetero-bi-functional [10,11]. Furthermore, another characteristic of S100 proteins is their binding to additional divalent metal ions such as Zn^{2+} and Cu^{2+}. Binding of these metals can affect the affinity to Ca^{2+}, further contributing to their variable cation binding properties and their diversified functions [9,12,13].

S100 proteins could act as a calcium mediated intracellular signal transducers through significant structural changes upon calcium binding, exposing two hydrophobic target-binding surfaces per dimer [14,15]. This behavior suggests that S100 proteins might have a role in the fine regulation of effectors' proteins, specific steps of signaling pathways, or cellular functions ranging from calcium buffering, cell growth and differentiation, modulation of enzyme activities, energy metabolism, motility, secretion, transcription, apoptosis, neurite extension and chemotaxis [10,16,17]. Lack of regulation of specific S100 proteins is correlated with several human diseases, including cancer, neurodegenerative and cardiovascular disorders [16]. The mechanism by which human S100A12 modulates the course of the inflammatory processes was linked to its interaction with the receptor for advanced glycated products (RAGE) [18]. Also, in a recent study, Xie et al. showed that the binding to this receptor occurs through a hexameric Ca^{2}-S100A12 C [19].

Porcine S100A12 (also known as calgranulin C) is a member of S100 proteins subfamily. This protein consists of 91 amino acids (approximately 10.7 kDa and an acid p*I* of 5.8) and is characterized by the presence of two EF-hands motifs and an additional binding site (His-X-X-X-His), with high affinity for Zn^{2+} on the C-terminal region [20]. The porcine S100A12 has a lower affinity to bind Ca^{2+} than Zn^{2+} and the ability for binding calcium is remarkably increased by the zinc

* Corresponding author. Grupo de Biofísica Molecular "Sérgio Mascarenhas", Centro de Biotecnologia Molecular Estrutural, Instituto de Física de São Carlos, CP 369, 13560-970 Universidade de São Paulo, São Carlos, SP, Brazil.
E-mail address: anapaula@ifsc.usp.br (A.P.U. Araújo).

0301-4622/$ – see front matter © 2008 Elsevier B.V. All rights reserved.
doi:10.1016/j.bpc.2008.02.013

binding [6,20]. Interestingly, Zn^{2+} binding to other S100 proteins like S100B [21] increases their affinity for Ca^{2+} (as occurs in S100A12) [22] whereas in S100A2 Zn^{2+} binding decreases its Ca^{2+} affinity.

Most S100 proteins are described by their three-dimensional struc2tures, but little is known about the pathway of protein folding/unfolding states [23]. In a previous study [20], spectroscopy tools were used to characterize the binding properties (of Ca^{2+} and Zn^{2+}) of native porcine S100A12 [20]. In the present work, we report a thermodynamic study focused on the structural stability and the folding/unfolding processes of the porcine S100A12 using far-UV circular dichroism (CD). The Ca^{2+} affinities in the presence of Zn^{2+} were also obtained using isothermal titration calorimetry (ITC). In addition, we show novel data for recombinant S100A12 (rS100A12) conformational changes induced by Ca^{2+} and Zn^{2+} binding resulting in the exposure of hydrophobic regions.

2. Materials and methods

2.1. Synthetic gene assembly and cloning

The gene sequence encoding porcine S100A12 was synthesized based on the protein amino-acid sequence [20], according to the *E. coli* codon bias [24]. The DNA coding sequence was formed by the overlap of the 3′ end using 10 pmol of the following primers (5′ GCT TCA GTT CAC GTT TGA TCA GGG TGT CGT AGT GAC CCA GAC GAA CAG AGT ACT GGT GGA AGA TG 3′, 5′ CAA ACG TGA ACT GAA GCA GCT GAT CAC CAA AGA ACT GCC GAA CAC CCT GAA GAA CAC CAA AGA CC 3′, 5′ CAT CTT GGT TAG CGT CCA GGT TCT GGA AGA TTT TGT CGA TGG TAC CCT GGT CTT TGG TGT TCT TC 3′, and 5′ GGA CGC TAA CCA AGA TGA ACA GGT TTC TTT CAA AGA ATT CGT AGT TCT GGT TAC TGA CGT ACT G 3′). This product, extended by the *Taq* DNA polymerase (Invitrogen), was used as template in a PCR to assemble the whole fragment. In this amplification reaction 100 pmol of each primer was used (5′ GGA ATT CCA TAT GAC CAA GCT GGA GGA CCA CCT GGA AGG TAT TAT CAA CAT CTT CCA CCA GTA CTC 3′, and 5′ GCC GCT CGA GTT CTT TGT GGA TGT TGT CGT GAG CGG TGA TCA GTA CGT CAG TAA CCA G 3′) for synthesis of the rS100A12 coding sequence. The PCR product was purified using the QIAquick PCR purification kit (QIAGEN, Hilden, Germany) and cloned into pGEM-T easy (Promega). The S100A12 coding sequence was cleaved with *Nde*I and *BamHI* restriction enzymes (New England Biolabs, Inc., MA, USA) and subcloned into pET-28a(+) and pET-29a(+) expression vectors (Novagen, Inc., WI, USA), to produce pS100A12-His and pS100A12 plasmids, respectively. The fidelity of the constructs was checked by sequencing the dideoxy chain termination method [25] using an ABI Prism 377 automated DNA sequencer (Perkin Elmer, CA, USA) following the manufacturer's protocol.

2.2. Recombinant S100A12 expression

The recombinant expression vectors were used to overproduce rS100A12 with or without histidine tail. Five hundred milliliter of LB medium, containing 30 μg/mL of kanamycin, was inoculated with 5 mL of a fresh overnight culture of *E. coli* BL21(DE3) (Novagen) harboring pS100A12 or S100A12-His (250 rpm at 37 °C). The cultures were induced by the addition 0.1 mM IPTG at OD_{600} of 0.8. Subsequently, the incubation temperature was decreased to 22 °C for around 12 h. Finally, the cells were harvested by centrifugation at 7000 ×*g* for 15 min at 4 °C.

2.3. Protein purification

The cell pellets were suspended in 10 mL of buffer 20 mM Tris–HCl (pH 8.0) containing 300 mM NaCl, lysed by sonication at 4 °C and the insoluble debris were separated by centrifugation at 14,000 ×*g* for 25 min. The purification of rS100A12 and rS100A12 with His-tag were performed by size exclusion and metal affinity chromatography, respectively.

The supernatant containing rS100A12 was loaded onto a Superdex-75 column (GE Healthcare) pre-equilibrated and eluted with 20 mM Tris–HCl pH 8.0 buffer containing 300 mM NaCl. Eluted fractions corresponding to rS100A12 (~11 kDa) were pooled and dialyzed against 20 mM Tris–HCl (pH 8.0). After dialysis, the sample was loaded onto a Mono Q HR 5/5 column (GE Healthcare), previously equilibrated with 20 mM Tris–HCl pH 8.0 (buffer A). The chromatography was performed on an ÄKTA Purifier (GE Healthcare) with a combination of two linear gradients of NaCl concentration (0–0.14 M in 20 min followed by 0.14–0.35 M in 15 min) in buffer A. The flow rate was 1 mL/min. S100A12 eluted at approximately 0.15 M NaCl and the protein purity was checked by Comassie stained 15% SDS-PAGE [26].

The supernatant containing the rS100A12 with His-tag, was loaded onto a Ni-NTA superflow column (4 mL, QIAGEN) pre-equilibrated with the same buffer used for cell suspension. The column was washed with 10 column volumes of sonication buffer and the target protein was eluted with five column volumes of the same buffer containing 250 mM imidazole. Samples from each step were analyzed on 15% SDS-PAGE. The protein samples were dialyzed against a 20 mM Tris–HCl buffer pH 8.0, containing 10 mM NaCl, before the assays.

Due to the high yield of protein containing His-tag, most experiments were carried out with this protein. The rS100A12 without His-tag was used only in the metals binding assays to eliminate the possibility of unspecific ion interactions.

2.4. Protein concentration

The concentration of recombinant proteins was determined by UV absorbance at λ = 280 nm (spectrophotometer U-2001 Hitachi) using a theoretical extinction coefficient based on the amino-acid composition [27]. The theoretical extinction coefficient employed was $\varepsilon_{280} = 2980\ M^{-1}\ cm^{-1}$.

2.5. Buffers and solutions

All chemicals and reagents, used in this study, were of the highest purity grade. To cover a pH range between 3 and 12, glycine–HCl (pH 3.0), sodium acetate–HCl (pH 4.0), MES–HCl (pH 6.0), Tris–HCl (pH 7.5–8.0), bicin–NaOH (pH 8.5), glycine–NaOH (pH10–10,5), were chosen as buffers and prepared at a final concentration of 20 mM containing 10 mM NaCl. The 8 M urea stock solution was prepared in 20 mM Tris–HCl pH 8.0 buffer containing 10 mM NaCl.

2.6. Oligomerization state

Chemical cross-linking was used to verify the oligomeric state of apo-rS100A12 by incubating the protein (10 μM) in presence of 20 mM HEPES pH 8.0 10 mM NaCl and DSS (50 mM) in a final reaction volume of 100 μL at 22 °C for 1 h. The reaction was quenched by the addition of 50 mM Tris–HCl, pH 7.5 and subsequently analyzed on SDS-PAGE. Size exclusion chromatography (SEC) was performed on an ÄKTA HPLC system using a Superdex-75 analytical size exclusion column equilibrated in 20 mM Tris–HCl pH 8.0 buffer containing 10 mM NaCl. Pre-equilibrated samples of apo-rS100A12 at concentrations between 10 μM and 25 μM were injected, and the relative elution volume was compared to that of molecular mass standards. The relative elution volume was calculated as: $K_{av} = (V_e - V_0)/(V_c - V_0)$, where V_e is elution volume, V_0 is the void volume, and V_g is the geometric column volume. A standard curve was plotted of K_{av} versus log(M). The molecular weight of apo-rS100A12 was estimated from the calibration curve.

2.7. Chemical unfolding/refolding of apo-rS100A12

The denaturation curves were taken in 20 mM Tris–HCl (pH 8.0), 10 mM NaCl and increasing concentration of urea from 0 to 7 M. Refolding of rS100A12 was done by quick protein dilution (1:50 fold)

against the same buffer with decreasing concentration of urea from 6 to 0 M and under gentle agitation [28]. The experiments were carried out in triplicate. The temperature of all experiments was maintained at 22 °C unless otherwise indicated.

2.8. Far-UV circular dichroism (CD)

Thermal and chemical unfolding of rS100A12, were monitored by far-UV CD spectroscopy using a JASCO J-715 instrument (JASCO Corporation, Japan) equipped with a Peltier temperature control unit. Far-UV circular dichroism (CD) measurements were performed using a cylindrical 0.1 cm path quartz curvet and the solvents spectra were subtracted in all experiments to eliminate background effects. CD spectra were the average of 16 accumulations, using a scanning speed of 100 nm min^{-1}, spectral bandwidth of 1 nm, and a response time of 0.5 s. The rS100A12 concentrations were 15, 25 and 50 μM. Thermal denaturation of rS100A12 was characterized by measuring the ellipticity changes at 220 nm induced by a temperature increase from 20 °C to 94 °C at a heating rate of 10 °C h^{-1}. Reversibility of rS100A12 denaturated was assessed, acquiring the CD spectra of the sample at the same initial condition after heating to 95 °C at 10 °C h^{-1}. Similarly, far-UV CD denaturation plots for the S100A12 folding/unfolding were obtained by measuring the ellipticity changes value at 220 nm induced by urea concentration.

2.9. Analysis of chemical denaturation

The ellipticity data obtained from the study of chemical denaturation of rS100A12 were analyzed assuming that this is a reversible two-state process. The fraction of denatured protein, f_D, is calculated from the relationship:

$$f_D = \frac{\theta_n - \theta_{obs}}{\theta_n - \theta_d} \quad \text{and} \quad f_n + f_d = 1 \tag{1}$$

in which θ_{obs} is the ellipticity of the sample at a particular condition; θ_d and θ_n are the values of ellipticity characteristic of the denatured and native states.

Chemical unfolding data were fit using a two-state homodimer model according Mallan et al. [29], in which two populations of protein exist at equilibrium, namely, folded homodimers (*D*) and unfolded monomers (*M*).

2.10. Fluorescence experiments (ANS assay)

Fluorescence emission measurements were performed on a spectrofluorimeter (ISS, IL, USA), model ISS K2, equipped with a refrigerated circulator (Neslab RTE-210). The excitation and emission monochromators were set at 2 and 1 nm slit widths, respectively. Fluorescent dye binding experiments with 1-anilino-8-naphthalene-sulfonic acid (ANS) were performed in order to probe dynamic changes and the exposure of hydrophobic regions of the protein [30]. A fixed concentration of ANS (250 μM) was mixed to the protein solution (10 μM, in 20 mM Tris–HCl pH 8.0 10 mM NaCl) in the presence or absence of Ca^{2+} or/and Zn^{2+} (1 mM final concentration). The excitation wavelength was set at 360 nm and the emission spectrum was monitored from 400 nm to 650 nm wavelength.

2.11. Isothermal titration calorimetry (ITC)

Isothermal titration calorimetry was carried out using a VP-ITC instrument from MicroCal (Northhampton, MA) at 25 °C in 20 mM Tris–HCl pH 8.0 buffer, containing 1 mM $ZnSO_4$. To investigate the binding of Ca^{2+} to rS100A12 in the presence of Zn^{2+}, 1 mM Ca^{2+} was titrated into 150 μM Zn^{2+}–S100A12 bound form. The experiment was repeated three times. The titration was performed by 45 injections of 10 μL each into the sample cell. The mixture was allowed to react for 120 s between injections. The injections were carried out over a 20 s period between each injection, which was sufficient for the baseline to be reestablished. The data obtained from isothermal titration were analyzed using the Origin software package for ITC analysis from Microcal (Microcal, Inc.). The data was fit using the sequential binding site model [31].

3. Results

3.1. Synthetic gene assembly, expression and purification of porcine rS100A12

The DNA coding sequence of the S100A12 protein was successfully obtained by the synthetic gene assembly and inserted into pET expression vectors. The target gene was expressed by the addition of 0.1 mM IPTG to the culture of *E. coli* BL21(DE3) harboring pS100A12 or pS100A12-His (Fig. 1).

The rS100A12 was purified by a two-step chromatographic protocol using size exclusion (SEC) followed by ion-exchange column.

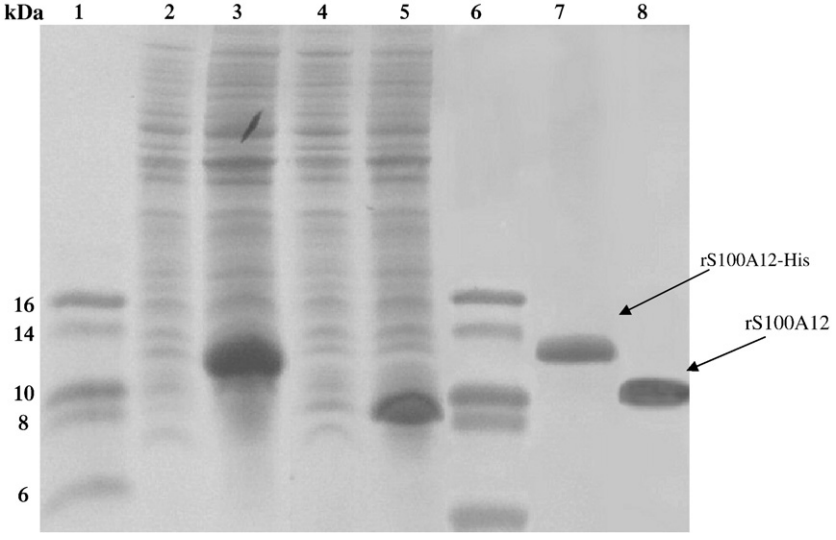

Fig. 1. Recombinant S100A12 expression and purification. Tricine/SDS-PAGE: (1 and 6) Low mass standard; (2–3 and 7) rS100A12 with His-tag; (4–5 and 8) rS100A12; (2 and 4) total proteins before induction; (3 and 5) after induction with 0.01 mM IPTG; (7) rS100A12 with His-tag purified on a Ni-NTA affinity column and (8) rS100A12 purified by an anion exchange column (mono-Q).

The rS100A12 with His-tag was purified using the Ni-NTA affinity chromatography (Fig. 1). The rS100A12 with and without His-tag yields were typically 160 and 60 mg of pure protein/liter of induced bacterial culture, respectively.

3.2. Determination of the oligomeric state of rS100A12

The oligomeric state of apo-rS100A12 was examined using SEC and cross-linking experiment at different protein concentrations. The apo-rS100A12 elutes from SEC as a single peak corresponding to an apparent molecular mass of approximately 29 kDa (Fig. 2). This indicated that apo-rS100A12 would be compatible with a homodimer in solution. The existence of a homodimer was confirmed by a cross-linking assay using DSS (inset, Fig. 2). The addition of divalent ions (Ca^{2+} or/and Zn^{2+}) did not change the oligomeric state of rS100A12 (data not shown).

3.3. Influence of pH on protein stability

Influence of pH on the secondary structure of the rS100A12 was studied using CD spectroscopy. Fig. 3A (solid line) shows the CD spectra of apo-rS100A12 at pH 8 and 20 °C, characterized by two negative bands at 222 nm and 208 nm. These bands are characteristic of protein containing α-helical elements in the secondary structure. The far-UV CD spectra of the protein at 20 °C under different pH (4, 5, 6, 7.5, 8.5, 9.5 and 10.5) was very similar to pH 8. Similar behavior was also observed with the tyrosine emission fluorescence at the above mentioned pH (data not shown).

3.4. Chemical stability studies

The apo-rS100A12 was denatured in 0 M to 7 M urea range at pH 8.0 and 20 °C in different protein concentrations (15, 25 and 50 μM). Fig. 3A shows the far-UV CD spectra and the negative ellipticities exhibited around 222 nm in the absence and presence of different urea concentrations. When the urea concentration was increased in the protein solution, a concomitant decrease in the ellipticity at 222 nm was observed, suggesting a cooperative loss of the α-helix content in apo-rS100A12. At 7.0 M urea a complete denaturation was observed, and the far-UV CD spectra was typical of a protein lacking secondary structure. On the other hand, the refolding of rS100A12 revealed that chemical denaturation by urea was a reversible process (Fig. 3B). Unfolded and subsequently refolded apo-rS100A12 retains approximately 90% of its native far-UV CD signal in the conditions described here.

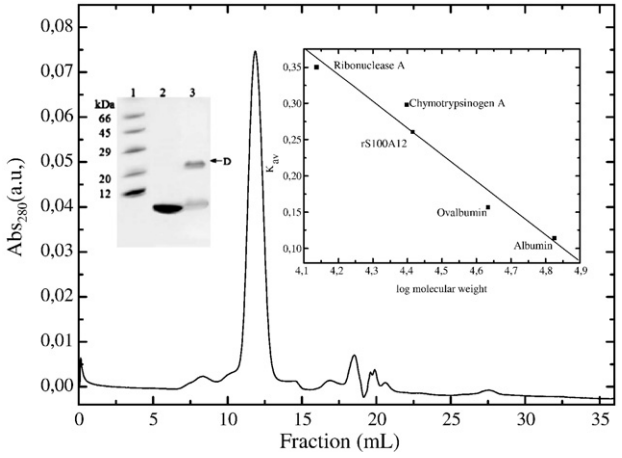

Fig. 2. Determination of the oligomeric state of rS100A12 by size exclusion chromatography (SEC). Conditions: room temperature in 20 mM Tris–HCl pH 8.0 buffer containing 10 mM NaCl. The two insets in the figure show the cross-linking reaction analyzed by tricine/SDS-PAGE and the calibration curve.

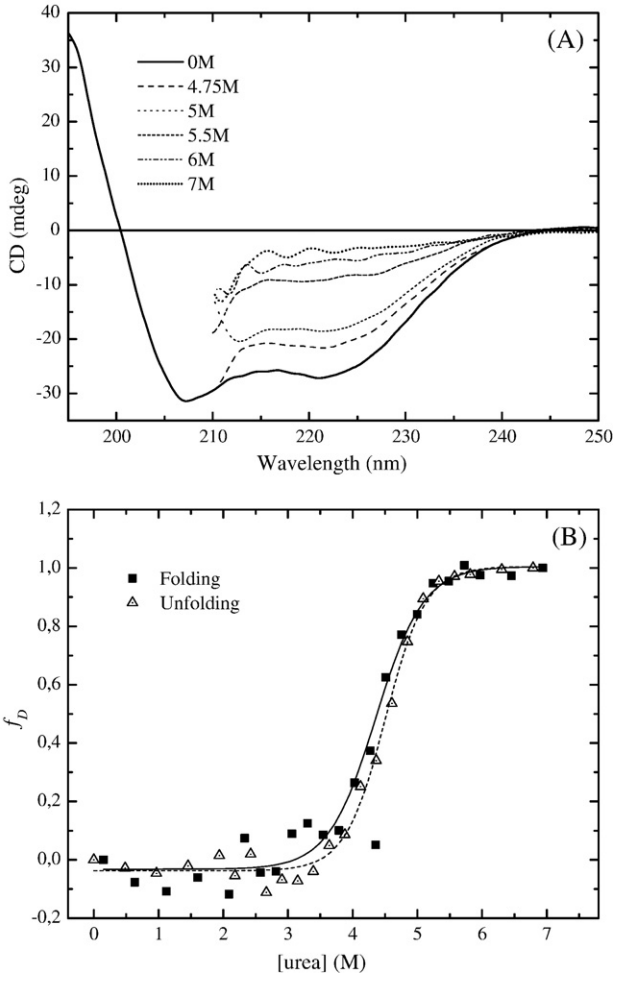

Fig. 3. Urea induced unfolding/folding of rS100A12 monitored by far-UV CD. (A) Urea concentrations were from top to bottom as follows: 7.0, 6.0, 5.5, 5, 4.75 and 0 M. (B) CD of rS100A12 as a function of urea concentration at pH 8. Urea-unfolding (r) and refolding (n) plots at 222 nm. The data have been normalized for ease of comparison. The conditions are described in material and methods.

Two-state homodimer denaturation model in which native homodimer (D) is in equilibrium with unfolded monomer (M) was used in this study. The far-UV CD data were treated and curves for each concentration of protein were fit individually using a two-state homodimer model according Mallan et al [29] (Supplementary material). Table 1 shows that for the far-UV CD data, $m_{N_2 \leftrightarrow 2D}$ and $\Delta G^{N_2 \leftrightarrow 2D}_{H_2O}$ remains similar for all protein concentrations used. $\Delta G^{N_2 \leftrightarrow 2D}_{H_2O}$ is the free energy difference between 1 mol of dimer and 2 mol of unfolded monomer in the absence of denaturant.

3.5. Apo-rS100A12 thermal unfolding study by CD

The nature of the thermal unfolding/refolding transition, in different protein concentrations, was studied by circular dichroism spectroscopy. Fig. 4 shows the family of temperature curves obtained

Table 1
Thermodynamics parameters (chemical unfolding) for the fit of apo-S100A12 equilibrium unfolding data to a two-state dimer denaturation model

	$P_{t\ (\mu M)}$	$\Delta G^{N_2 \leftrightarrow 2D}_{H_2O}$ (kg mol^{-1})	$m_{N_2 \leftrightarrow 2D}$ (kJ mol^{-1} M^{-1})	$[U]_{1/2}$ (M)
apo-rS100A12	15	93.8±5.6	9.9±0.9	4.7
apo-rS100A12	25	89.2±4.3	9.6±0.9	4.5
apo-rS100A12	50	83.3±4.0	9.2±0.7	4.2

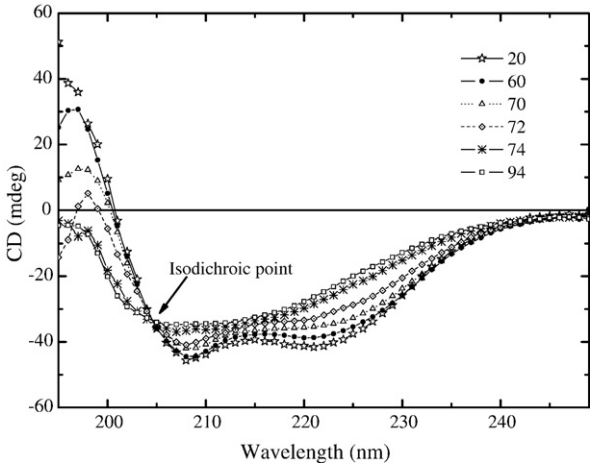

Fig. 4. Recombinant S100A12 thermally unfolding monitored by far-UV CD. Spectra were measured in 20 mM Tris–HCl (pH 8.0) containing 10 mM NaCl. The isodichroic point can be observed at ~204 nm. Temperatures were from top to bottom as follows: 94, 74, 72, 70, 60, and 20 °C. The data have been normalized for ease of comparison (the experimental conditions are described in Materials and methods).

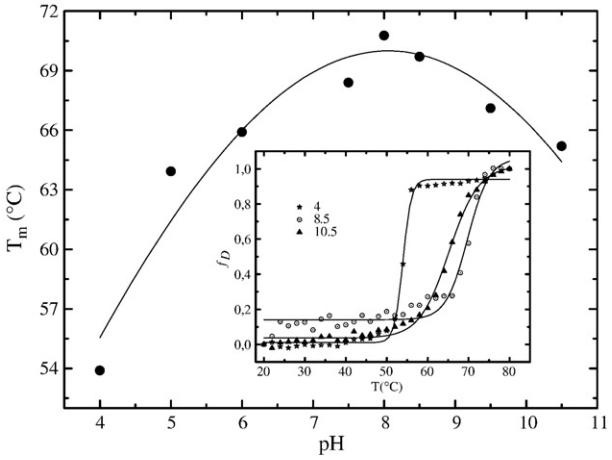

Fig. 6. pH dependence of rS100A12 thermal stability. Dependence of T_m as a function of pH, values obtained by far-UV CD in the pH range of 4.0–10.5. The inset figure shows the f_D as a function of temperature in the pHs 4, 8.5 and 10.5.

at 15 μM of protein, pH 8.0. The well-defined isodichroic point can be observed at 204 nm (Fig. 4). The thermal unfolding/refolding of apo-rS100A12 was monitored following changes in the CD ellipticity at 222 nm as a function of the temperature and exhibited a cooperative sigmoidal behavior (Fig. 5). When the temperature was increased from 20 °C up to 94 °C, the far-UV CD spectra of apo-rS100A12 showed a decrease in the overall ellipticity. Apo-rS100A12 after unfolded and subsequently refolded (cooling back to 20 °C) retains approximately 80% of initial far-UV CD signal (data not show).

3.6. Metal binding influence on rS100A12 stability

We performed thermal unfolding studies by far-UV CD (Fig. 5) in the presence of Zn^{2+} and Ca^{2+} in order to investigate the conformational states induced by these ions on apo-rS100A12. The melting temperature value for apo-rS100A12 was calculated and resulted in T_m=68.4 °C. However, the addition of 1 mM Zn^{2+} to the apo-rS100A12 greatly increased its stability, where T_m was 84 °C. The same effect was verified if the thermal unfolding was carried out in the presence of Ca^{2+} (1 mM), showing a T_m for the Ca^{2+}-bound rS100A12 of 79 °C (Fig. 5).

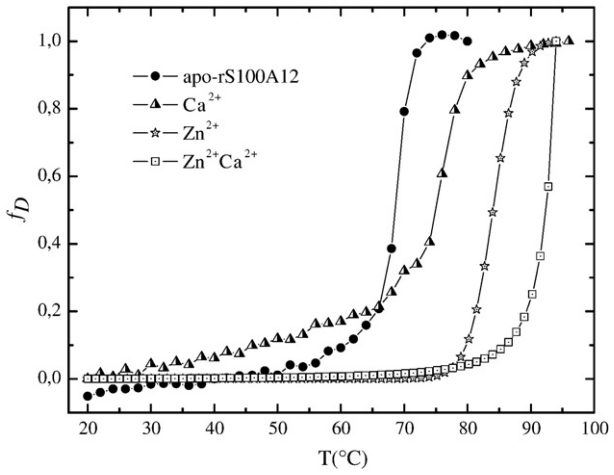

Fig. 5. Influence of Zn^{2+} and Ca^{2+} on thermal stability of rS100A12 monitored by far-UV CD. (●) Apo-S100A12, (A) Zn^{2+}, (▲) Ca^{2+} and (□) $Zn^{2+}Ca^{2+}$ loaded forms. The data have been normalized for ease of comparison. The conditions are described in material and methods.

The addition of 1 mM Ca^{2+} to Zn^{2+}-bound rS100A12 induced a higher increase in the protein thermal stability, preventing the complete unfolding of the rS100A12 in the conditions described here (Fig. 5).

The thermal and chemical unfolding results showed a significant increase on rS100A12 stability in the presence of both ions. The urea concentration in which 50% of rS100A12 molecules are in the denatured state(s) was 1 M higher than the observed for the apo-rS100A12 (data not shown). Taken together, the results indicate that the chemical unfolding results match the thermal unfolding experiments and suggest that the final conformational stability of rS100A12 is dependent of the metal ions and the nature of the ion.

3.7. Influence of pH on apo-rS100A12 stability

Temperature unfolding of apo-rS100A12 was characterized at different pH values. At 20 °C, the results showed that the CD spectra in the pH range (4.0–10.5) were in agreement, considering the experimental error, with those observed in Fig. 4. These results exclude any effect of pH on the secondary structure of apo-rS100A12 at 20 °C. Nevertheless, the apo-rS100A12 thermal stability was found to be pH-dependent. The melting temperature remains almost constant between pH 7.0 and 9.0, but the thermal stability was reduced in pH lower than 6.0 and higher than 8.0 (see Fig. 6).

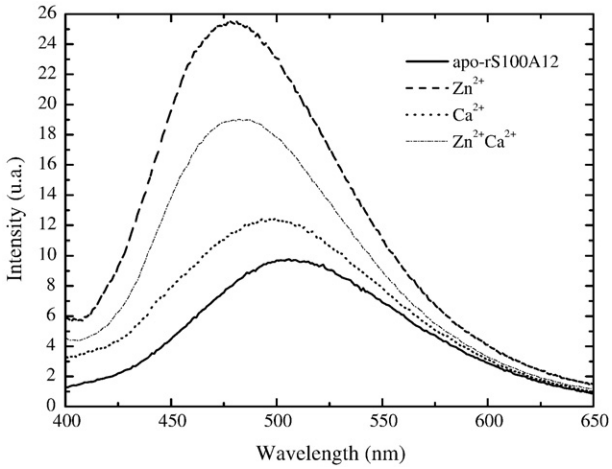

Fig. 7. ANS assays of the apo-rS100A12, Zn^{2+}, Ca^{2+} and $Zn^{2+}Ca^{2+}$ loaded forms. The figure shows the increasing in fluorescence intensity of ANS upon metal addition.

3.8. ANS binding studies

The dye ANS, an extrinsic fluorescence probe, was used to investigate the affinity of ions binding to rS100A12. ANS has been successfully used to detect solvent-accessible hydrophobic surface in proteins [30]. The ANS fluorescence emission was monitored in the presence of Zn^{2+}, Ca^{2+} or the combination of Zn^{2+} and Ca^{2+}. Fig. 7 (solid line) shows ANS spectra with apo-rS100A12 at 20 °C. The Ca^{+2} addition resulted in an increase of the ANS maximum intensity emission and a blue shift (Fig. 7). Similar results were observed in the presence of Zn^{2+}, but with higher emission intensities. On the other hand, the addition of both ions showed similar emission spectra to that of the apo-form. The results above indicated that the Ca^{2+} or Zn^{2+} in Zn-rS100A12 leads to an exposition of hydrophobic regions on the protein surface. When similar experiments were done with refolded protein (in the presence or absence of divalent ions) similar results were obtained, indicating that the refolded protein was able to bind ions and suggesting that it was biologically active.

3.9. Isothermal titration calorimetry (ITC)

The interaction of Ca^{2+} with Zn^{2+}-S100A12 was studied using high sensitivity ITC. Fig. 8 shows the isothermal titration curve obtained by the interaction between Zn^{2+}-rS100A12 and Ca^{2+}. Best-fit of the binding isotherm yields apparent binding constant values in the order of 10^7 M^{-1} and 10^4 M^{-1}. That was consistent with what was described by Dell´Angellica et al. for the native porcine S100A12 using emission fluorescence spectroscopy [20].

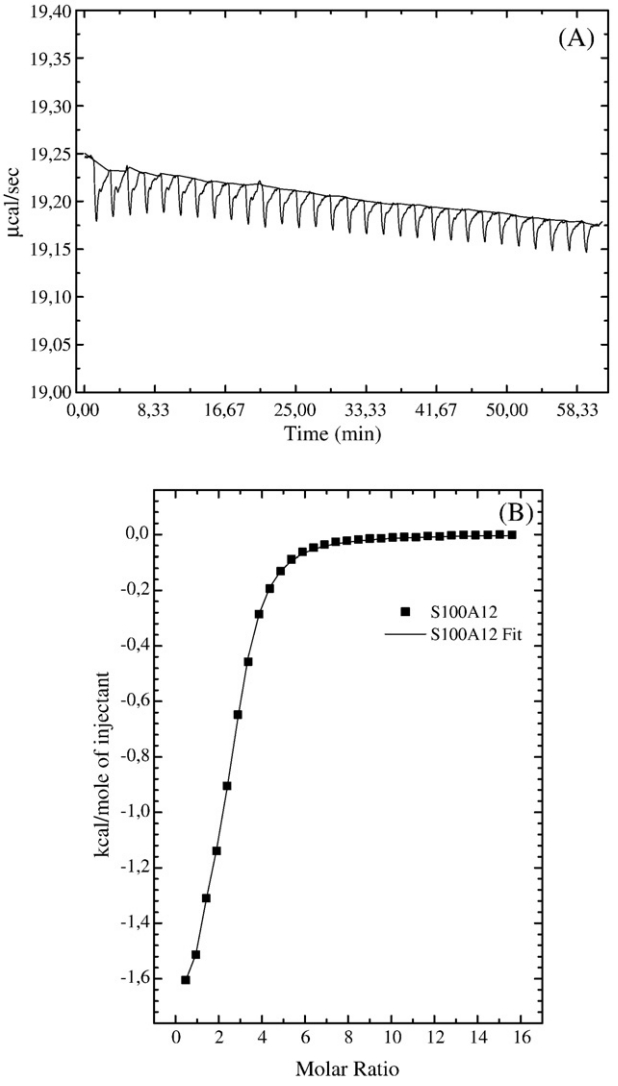

Fig. 8. Isothermograms representing the binding of Ca^{2+} to Zn^{2+}-S100A12. The upper panel represents the raw data and the bottom is the best-fit of the raw data. The binding isotherms have been fit to the two binding sites model. The concentration of protein used was 150 µM in 20 mM Tris/HCl (pH 8) containing 10 mM NaCl at 25 °C.

4. Discussion

Studies involving heterologous expression proteins in *E. coli* revealed that when the protein is relatively small, the final yield of production is improved [33]. Thus, the production of porcine S100A12 by heterologous expression strategy was successful and an interesting approach, resulting in large amount of fully active protein.

Particular attention has recently been given to S100 proteins, since several members of this family were reported to bind Ca^{2+} and some transition metals like Cu^{2+} and Zn^{2+} [10]. But little is known about the mechanism and function induced by the binding of these intracellular transition metals to the S100 proteins. In this study, we have used far-UV CD and fluorescence spectroscopy to demonstrate that rS100A12 can specifically bind Ca^{2+} or/and Zn^{2+}, and in doing so, these metal ions induced conformational changes in the protein leading to an increased structural stability (chemical and thermal).

The native S100A12 was described as a homodimer in solution [20]. Size exclusion chromatography (SEC) and cross-linking experiments were used to confirm the oligomeric state of recombinant apo-S100A12 in solution (Fig. 2) over a range of protein concentrations (10–50 µM). Results of both techniques were consistent with a stable homodimer. The addition of metals (Ca^{2+} or/and Zn^{2+}) did not affect the oligomeric state of rS100A12. In contrast, human S100A12, which shares 70% sequence identity with porcine S100A12, forms a trimer of dimers in high-calcium concentration [32,34]. The hexamer observed for human protein possesses additional calcium ions coordinated by the side chain oxygens of residues from two adjacent dimers (Gln58, Gln64 and Glu55) and are considered necessary for hexamer formation [6]. The porcine rS100A12 exhibited a Lys55 instead of Glu55, which could hinder the additional calcium coordination requested for hexamerization. Similarly, bovine S100A12 shows two Lys residues instead of Glu55 and Gln64 and, as porcine S100A12, is unable to assemble in a hexamer.

The structural stability of apo-rS100A12 was analyzed, using far-UV CD spectroscopy, by urea denaturation, over a large range of protein concentrations. The curves suggest that no intermediates are present in detectable amounts during unfolding transition. Also, we show that chemical unfolding transition was very nearly completely reversible (~90%) upon removal of the denaturing condition (Fig. 3A and B). The data were analyzed using a two-state model in which two protein populations exist at equilibrium, namely, folded homodimers (D) and unfolded monomers (M). The protein concentration-dependence of equilibrium unfolding curves in homodimer systems is expected, and can be rationalized from the way the equilibrium constant K_U is defined: $K_U=[M]^2/[D]$. At a given denaturant concentration, K_U and ΔG remain constant for all protein concentrations, and only the fraction of each equilibrium species present change with P_t. In a homodimeric system, $[U]_{1/2}$ is defined as the concentration of denaturant where the fraction of unfolded monomers is equal to the fraction of monomers present as dimers. This is also where $K_U=P_t$, therefore, the concentration of denaturant where $[U]_{1/2}$ occurs will depend of P_t, and a change in $[U]_{1/2}$ with the total protein concentration is expected. $\Delta G^{N_2 \leftrightarrow 2D}_{H_2O}$ remains the same with changing P_t and $[U]_{1/2}$. The m value is a constant for each protein and should not be affected by protein concentration. When apo-rS100A12 unfolding data were analyzed according to a two-state denaturation model, $m_{N_2 \leftrightarrow 2D}$ and $\Delta G^{N_2 \leftrightarrow 2D}_{H_2O}$ values remain similar (Table 1 and Supplementary material) for all concentrations of the protein used (within experimental error of 10%).

Thus, a two-state homodimeric model described the experimental results adequately. However, the dimeric form of S100A12 probably

can dissociate producing monomers before reaching the denatured state. It is interesting that these forms could not be detected by the methods used in the present work. Analysis using intrinsic fluorescence also suggested that S100A12 unfolding occurs via a two-state transition without intermediate species (data not shown).

The thermal unfolding/refolding of apo-rS100A12 was monitored using far-UV CD spectroscopy. When the temperature was increased from 20 °C to 94 °C, the shape of the far-UV CD spectra of apo-rS100A12 revealed a decrease in the overall ellipticity and the presence of an isodichroic point at 204 nm (Fig. 4). These results point to a cooperative loss of the α-helix structure of apo-rS100A12 and to a two-state homodimer transition (as expected for a system in which only two conformations are present). The content of α-helix is maximal at temperature below the transition and decreases to zero at temperatures above the transition region. The apo-rS100A12 denaturation was nearly completely reversible in the conditions used, since samples that were heated above 90 °C return to approximately 80% their original state when allowed to cool slowly to 20 °C.

Our results show that there are no structural changes in apo-rS100A12 within the pH range of 4.0–10.5 at 20 °C. However, a thermal pH dependence of apo-rS100A12 was observed. The stability of apo-rS100A12 decreases at pH values below 6.0 and above 9.0, remaining constant at pH values comprised between 7 and 9. The kinetic unfolding in several pHs allowed us to calculate the melting temperature T_m of apo-rS100A12 for each pH value (Fig. 6). The maximum stability of apo-rS100A12 is wider than the narrow physiological pH range.

Thermodynamic analysis of the interactions of Zn^{2+}, Ca^{2+} or Zn^{2+} and Ca^{2+} with apo-rS100A12 indicated that these metals enhance the structural stability of the protein (Fig. 5). The melting temperature of apo-rS100A12 occurs at 68.4 °C. The thermal stability of apo-rS100A12 showed significant increases after Zn^{2+} or Ca^{2+} addition (84 °C and 79 °C, respectively). Interestingly, the binding of zinc raised the thermal stability of Ca^{2+}-loaded rS100A12. The binding of these metals may be essential to induce conformational changes exposing hydrophobic patches, thus facilitating the interaction with a hydrophobic region of the secondary effectors protein [10,16,33].

The ANS fluorescence results suggested the apo-S100A12 has a low amount of exposed hydrophobic surface area (Fig. 7). The addition of Ca^{2+} results in an increase in the emission intensity of the ANS suggesting a conformational change as observed to CaBPs [35]. This result is consistent with that observed in other S100 proteins, were the Ca^{2+}-binding results in an increase in the solvent accessibility of non-polar residues [33]. Ca^{2+}-bound states of S100 proteins recognize and bind to their target proteins through the solvent-exposed hydrophobic surfaces [4,33]. Our results suggest that rS100A12's mechanism of activation and recognition of target protein may be the same from other members of the S100 protein family. ANS binds more strongly in the Zn^{2+}-rS100A12 which leads to a large conformational change (Fig. 7). The increase in emission intensity is accompanied by a great blue shift in the ANS emission from 508 nm to 478 nm, indicating a hydrophobic surface exposition. The exposure of solvent-accessible hydrophobic patches was higher in the Zn^{2+}-bound state than that observed in the apo-rS100A12, Ca^{2+}-rS100A12 or $Zn^{2+}Ca^{2+}$-rS100A12. These findings possibly mean that structural changes influenced by Zn^{2+} and Ca^{2+} have a potential role in modulating the protein function.

Structural stability and biological activity correlations can be used to establish the mechanism of refolding. ANS binding experiments performed with refolded rS100A12 resulted in a similar profile that was exhibited by the native protein, which indicated that both thermal and chemical rS100A12 denaturations were reversible in the conditions assayed.

Since the binding of Zn^{2+} to S100A12 triggers a drastic conformational change and increases Ca^{2+} binding affinity to the protein, we performed ITC experiments to examine whether or not the rS100A12 retains such binding affinity to Ca^{2+} and Zn^{2+} (Fig. 8). The binding between Zn^{2+}-rS100A12 and Ca^{2+} is an exothermic process and the reaction proceeds with a negative change in enthalpy. Binding isotherm representing the Ca^{2+} titration shows that these ions interacted with the Zn^{2+}-rS100A12 loaded form with the same stoichiometric binding constants ($10^7\ M^{-1}$ and $10^4\ M^{-1}$) as those observed previously for the native S100A12 using fluorescence spectroscopy [20].

5. Conclusions

Our results show that equilibrium unfolding/refolding of recombinant S100A12 induced by urea or temperature proceeds by a reversible classical two-state homodimeric mechanism without the accumulation of intermediates. ANS experiments showing that the refolded rS100A12 regained the binding affinity to Zn^{2+} and Ca^{2+} lead us to propose that the biological activity was recovered. The structural stability was significantly increased in the presence of Zn^{2+} and Ca^{2+}. The metal influence on the structure of rS100A12 was also observed by ANS fluorescence indicating a large conformational change. The exact role for S100A12 has not yet been defined. In this sense, our studies provide a direction to understand the relation between structure stability, ions binding and the influence of these aspects on the biological function of S100A12. The interaction with different ions could be consistent with their physiological role in modulating the functional properties of S100A12 as the recognition of target proteins.

Acknowledgments

We would like to thank Prof. Leila Maria Beltramini for helpful discussions. We wish to thank the Fapesp, CNPq and Capes for financial support.

Appendix A. Supplementary data

Supplementary data associated with this article can be found, in the online version, at doi:10.1016/j.bpc.2008.02.013.

References

[1] R.M. Tufty, R.H. Kretsinger, Troponin and parvalbumin calcium binding regions predicted in myosin light chain and T4 lysozyme, Science 187 (1975) 167–169.
[2] R.H. Kretsinger, C.E. Nockolds, Carp muscle calcium-binding protein: II — structure determination and general description, J. Biol. Chem. 248 (1973) 3313–3326.
[3] R. Donato, S100: a multigenic family of calcium-modulated proteins of the EF-hand type with intracellular and extracellular functional roles, Int. J. Biochem. Cell Biol. 33 (2001) 637–668.
[4] L.S. Kisiel, A.C. Rintala-Dempsey, G.S. Shaw, Calcium-dependent and -independent interactions of the S100 protein family, Biochem. J. 396 (2006) 201–214.
[5] T. Hatakeyama1, M. Okada1, S. Shimamoto1, Y. Kubota, R. Kobayashi, Identification of intracellular target proteins of the calcium-signaling protein S100A12, Eur. J. Biochem. 271 (2004) 3765–3775.
[6] O.V. Moroz, G.G. Dodson, K.S. Wilson, E. Lukanidin, I.B. Bronstein, Multiple structural states of S100A12: a key to its functional diversity, Microsc. Res. Tech. 60 (2003) 581–592.
[7] B.C. Potts, J. Smith, M. Akke, T.J. Macke, K. Okazaki, H. Hidaka, D.A. Case, W.J. Chazin, The structure of calcyclin reveals a novel homodimeric fold for S100 Ca(2+)-binding proteins, Nat. Struct. Biol. 2 (1995) 790–796.
[8] R. Donato, Functional roles of S100 proteins, calcium-binding proteins of the EF-hand type, Biochim. Biophys. Acta 1450 (1999) 191–231.
[9] C.W. Heizmann, J.A. Cox, New perspectives on S100 proteins: a multi-functional Ca (II)-, Zn(II)- and Cu(II)-binding protein family, BioMetals 11 (1998) 383–397.
[10] D.C. Hilt, D. Kligman, The S-100 protein family: a biochemical and functional overview, in: C.W. Heizmann (Ed.), Novel Ca^{2+}-binding Proteins. Fundamentals and Clinical Implications, Springer Verlag, Berlin, 1991, pp. 65–103.
[11] J. Krebs, M. Quadroni, L.J. Van Eldik, Dance of the dimers, Nat. Struct. Biol. 2 (1995) 711–714.
[12] C.K. Wang, R.S. Mani, C.M. Kay, H.C. Cheung, Conformation and dynamics of bovine brain S100a protein determined by fluorescence spectroscopy, Biochemistry 31 (1992) 4289–4295.
[13] G. Zolese, I. Giambanco, G. Curatola, G. De Stasio, R. Donato, Time-resolved fluorescence of S100a protein in absence and presence of calcium and phospholipids, Biochim. Biophys. Acta 1162 (1993) 47–53.

[14] W.J. Chazin, Releasing the calcium trigger, Nat. Struct. Biol. 2 (9) (1995) 707–710.
[15] S.P. Smith, G.S. Shaw, A change-in-hand mechanism for S100 signalling, Biochem. Cell. Biol. 76 (1998) 324–333.
[16] C.W. Heizmann, G. Fritz, B.W. Schafer, S100 proteins: structure, function and pathology, Front. Biosci. 7 (2002) 1356–1368.
[17] J. Edgeworth, M. Gorman, R. Bennett, P. Freemont, N. Hogg, J. Biol. Chem. 266 (1991) 7706–7713.
[18] M.A. Hofmann, S. Drury, C. Fu, W. Qu, A. Taguchi, Y. Lu, C. Avila, N. Kambham, A. Bierhaus, P. Nawroth, RAGE mediates a novel proinflammatory axis: a central cell surface receptor for S100/calgranulin polypeptides, Cell 97 (1999) 889–901.
[19] J. Xie, D.S. Burz, W. He, I.B. Bronstein, I. Lednev, A. Shekhtman, Hexameric calgranulin C (S100A12) binds to the receptor for advanced glycated end products (RAGE) using symmetric hydrophobic target-binding patches, J. Biol. Chem. 282 (2007) 4218–4231.
[20] E.C. Dell'Angelica, C.H. Schleicher, J.A. Santome, Primary structure and binding proteins of cargranulin C, a novel S100-like calcium-binding protein from pig granulocytes, J. Biol. Chem. 269 (1994) 28929–28936.
[21] T. Ostendorp, C.W. Heizmann, P.M. Kroneck, G. Fritz, Purification, crystallization and preliminary X-ray diffraction studies on human Ca^{2+}-binding protein S100B, Acta Crystallogr. 61 (2005) 673–675.
[22] M. Koch, S. Bhattacharya, T. Kehl, M. Gimona, M. Vasák, W. Chazin, C.W. Heizmann, P.M. Kroneck, G. Fritz, Implications on zinc binding to S100A2, Biochim. Biophys. Acta, Mol. Cell Res. 1773 (2007) 457–470.
[23] C. Duy, J. Fitter, How aggregation and conformational scrambling of unfolded states govern fluorescence emission spectra, Biophys. J. 90 (2006) 3704–3711.
[24] P.R. Carey, Protein Engineering and Design, Academic Press, 1996, pp. 75–90.
[25] F. Sanger, S. Nicklen, R. Coulson, DNA sequencing with chainterminating inhibitors, Proc. Natl. Acad. 74 (1977) 5463–5467.
[26] K. Laemmli, Cleavage of structural proteins during the assembly of the head of bacteriophage T4, Nature 227 (1970) 680–685.
[27] S.C. Gill, P.H. von Hippel, Calculation of protein extinction coefficients from amino acid sequence data, Anal. Biochem. 182 (1989) 319–326.
[28] M. Sharon, Price C. Kelly, Nicholas, The application of circular dichroism to studies of protein folding and unfolding, Biochim. Biophys. Acta 1338 (1997) 161–185.
[29] A.L. Mallam, S.E. Jackson, Folding studies on a knotted protein, J. Mol. Biol. 346 (2005) 1409–1421.
[30] G.V. Semisotnov, N.A. Rodionova, O.I. Razgulyaev, V.N. Uversky, A.F. Gripas, R.I. Gilmanshin, Study of the "molten globule" intermediate state in protein folding by a hydrophobic fluorescent probe, Biopolymers 31 (1991) 119–128.
[31] V. Sivaraja, T.K.S. Kumar, D. Rajalingam, I. Graziani, I. Prudovsky, C. Yu, Copper binding affinity of S100A13, a key component of the FGF-1 non-classical copper-dependent release complex, Biophys. J. 91 (2006) 1832–1843.
[32] L.P. Miranda, T. Tao, A. Jones, I. Chernushevich, K.G. Standing, C.L. Geczy, P.F. Alewood, Total chemical synthesis and chemotactic activity of human S100A12 (EN-RAGE), FEBS Lett. 488 (2001) 85–90.
[33] O.V. Moroz, A.A. Antson, G.N. Murshudov, N.J. Maitland, G.G. Dodson, K.S. Wilson, I. Skibshoj, E.M. Lukanidin, I.B. Bronstein, The three-dimensional structure of human S100A12, Acta Crystallogr., D Biol. Crystallogr. 57 (2001) 20–29.
[34] H. Pessen, T.F. Kumosinski, Measurements of protein hydration by various techniques, Methods Enzymol. 117 (1985) 219–255.
[35] A.P.A. Pinto, P.T. Campana, L.M. Beltramini, A.M. Silber, A.P.U. Araújo, Structural characterization of a recombinant flagellar calcium-binding protein from Trypanosoma cruzi, Biochim. Biophys. Acta 1652 (2003) 107–114.